14th International Conference on Structural Safety and Reliability - ICOSSAR'25
1-6 June, 2025 - Los Angeles California, USA
R. Ghanem, E. Johnson, S. Masri and A. Olivier (Eds)

SENSITIVITY ANALYSIS OF HYDRODYNAMIC JOURNAL BEARING FAILURE MODES DUE TO LUBRICANT CONTAMINATION

HAYKAL BOUAJILA[1,3], YOUNES AOUES[2], JEAN BOUYER[1], PASCAL JOLLY[1], BALINT PAP[3] AND JAMES COLE[3]

[1] Institut Pprime, GMSC department, CNRS - University of Poitiers
F-86360 (Cedex), Chasseneuil-du-Poitou, France
Haykal.bouajila@univ-poitiers.fr, https://pprime.fr/

[2] INSA Rouen Normandie, Normandy University, LMN UR3828
F-76000 (Cedex), Rouen, France
Younes.aoues@insa-rouen.fr, https://www.insa-rouen.fr/

[3] Safran Transmission Systems
F-92707 (Cedex), Colombes, France
Haykal.bouajila@safrangroup.com, https://www.safran-group.com/fr/societes/safran-transmission-systems

Key words: Sensitivity analysis, Screening, Scratched plain bearings, Aerospace gearboxes

Abstract. This study focuses on the sensitivity analysis of failure modes in an hydrodynamic journal bearing, taking into account lubricant oil contamination. Two sensitivity analysis methods are employed to investigate hydrodynamic (HD) performance in the presence of a circumferential scratch on the shaft surface. The Morris method considers multiple input parameters of the numerical bearing model. A One-At-a-Time (OAT) design of experiments is used to evaluate the model's performance. The analysis classifies the parameters into three groups: those with nonlinear effects and strong interactions, those with linear and moderate effects, and those with negligible impact.

The second method is based on variance decomposition and the calculation of Sobol indices, using a Kriging surrogate model built from a Latin Hypercube Sampling (LHS) design. The results obtained from both methods help reduce the stochastic dimensionality of the hydrodynamic bearing reliability problem by treating the least influential parameters as deterministic. The study focuses on the variability of the key factors that significantly affect the minimum lubricant film thickness and the maximum pressure in the bearing.

1 INTRODUCTION

Hydrodynamic journal bearings are essential components in aerospace and energy systems, prized for their high reliability and ability to ensure full separation between the shaft and bearing surface under hydrodynamic lubrication. This separation reduces wear and extends service life. However, in real operating conditions, abrasive particles—originating from internal wear or external contamination—can infiltrate the lubricant. These particles often become embedded in the bearing lining, causing circumferential scratches on the shaft and degrading bearing performance.

Although the impact of such defects has been explored through flash temperature estimation[1], numerical simulations of scratched bearings[2], and experimental studies on thermo-mechanical behavior[3], most investigations adopt a deterministic approach. They generally overlook the variability and uncertainty in key parameters such as operating conditions (e.g., load, speed), lubricant properties (e.g., viscosity, temperature, cavitation pressure), and bearing geometry (e.g., L/D ratio, clearance, groove design). As a result, a comprehensive understanding of scratch-induced degradation on bearing reliability remains limited.

In this study, we address this gap by applying two complementary sensitivity analysis techniques. The Morris method, based on one-at-a-time (OAT) perturbations, is used for preliminary screening, while a global variance-based approach relying on Sobol indices quantifies parameter influence in a more detailed way. A kriging surrogate model is built from a Latin Hypercube Sampling (LHS) design to enable the Sobol analysis efficiently. Together, these methods identify the most influential parameters affecting bearing performance and enable a reduction in model dimensionality. This contributes to a more robust reliability assessment and improves the prediction of remaining useful life for hydrodynamic journal bearings in next-generation aircraft transmission systems.

2 AERONAUTICAL HYDRODYNAMIC JOURNAL BEARINGS

2.1 Hydrodynamic Journal Bearings

Hydrodynamic journal bearings are critical components in rotating machinery, providing precise radial support and guidance for rotating shafts. They are particularly well-suited for applications involving high rotational speeds and heavy loads, such as in the automotive industry, nuclear power systems, wind turbine gearboxes, turbochargers, and aircraft engines. Their main advantage lies in their ability to operate under HD lubrication conditions, which ensures minimal wear of the contacting surfaces throughout the machine's operational lifetime.

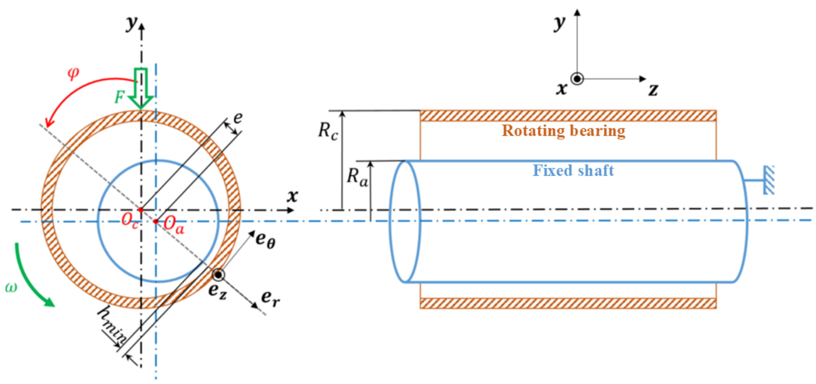

Figure 1: Schematic of a hydrodynamic journal bearing with rotating bushing and fixed shaft.

Unlike rolling-element bearings, hydrodynamic journal bearings have a simple design, consisting of only two components: a rotor (the rotating element) and a stator (the stationary element). In Figure 1, the bearing is depicted with a rotating bushing (bearing), having a center O_c and a radius

R_c, and a fixed shaft (journal), with a center O_a and radius R_a. The distance O_cO_a defines the absolute eccentricity e, while the angle φ, formed between the load direction (here aligned with the $-y$ axis) and the oil wedge axis (represented by $\overline{O_cO_a}$), corresponds to the angle of attitude. This angle identifies the position of the minimum film thickness within the active region of the bearing. Assuming an ideal and perfectly aligned bearing geometry (i.e., no misalignment and no surface scratches), knowing these two parameters e and φ is sufficient to determine the relative position of the stator relative to the rotor under various lubrication regimes. Consequently, the fluid film thickness can be defined using the following equation:

$$h = C(1 + \cos(\theta)\,\varepsilon) \tag{1}$$

Where, h is the thickness of the fluid film between the shaft and the bushing; C is the radial clearance, defined as $C = R_c - R_a$; ε is the relative eccentricity, defined as $\varepsilon = e/C \in [0, 1]$; θ is the circumferential coordinate (in radians); and e is the absolute eccentricity.

Based on the experimental work of Beauchamp Tower [4] and Petrov [5], Reynolds [6] derived an equation that describes the pressure distribution within a journal bearing operating under hydrodynamic lubrication. This equation—known as the **Reynolds equation**—is derived from the Navier-Stokes equations and the principle of mass conservation, and serves as the fundamental basis for the study of lubricated bearings.

Various forms of the Reynolds equation can be found in the literature, incorporating additional effects such as thermal phenomena, elastic deformation of the surfaces, or surface roughness. However, its classical form is expressed as follows:

$$\frac{1}{R}\frac{\partial}{\partial\theta}\left(\frac{h^3}{\mu}\frac{\partial p}{\partial\theta}\right) + \frac{\partial}{\partial z}\left(\frac{h^3}{\mu}\frac{\partial p}{\partial z}\right) = 12\omega\frac{\partial h}{\partial\theta} \tag{2}$$

Where R is the nominal radius of the bearing (m); μ is the dynamic viscosity of the lubricant (Pa·s); z is the axial coordinate (m); p is the pressure in the lubricant film (Pa); and ω is the angular velocity of the shaft (rad/s). Thus, Equation (2) is a second-order partial differential equation of elliptic type, where the unknown is the pressure field p of the lubricating film within the bearing.

At start-up, the bearing undergoes a critical phase due to high contact pressure and low rotational speed. Initially, the absence of lubrication leads to direct contact between the shaft and the bearing shell, characterizing a boundary lubrication regime. Then, as oil is gradually introduced, a mixed lubrication regime develops, with localized rotor-stator surface contacts being maintained. These two phases are the most conducive to wear. As the sliding speed and the clearance between the relatively moving surfaces (shaft and bearing) increase, the hydrodynamic regime takes over. The resulting oil film then ensures complete separation of the surfaces, theoretically eliminating direct contact and reducing wear to zero.

Under extreme conditions (i.e., high speed and temperature rise), the viscosity of the oil decreases due to shear, thereby altering its lubricating properties. Moreover, scratches caused by abrasive particles modify the distribution of the oil film. Therefore, evaluating the bearing's performance requires solving Reynolds equation (2) while accounting for surface roughness, lubricant properties, and the geometric parameters of the scratches (dimensions, position, shape, and quantity).

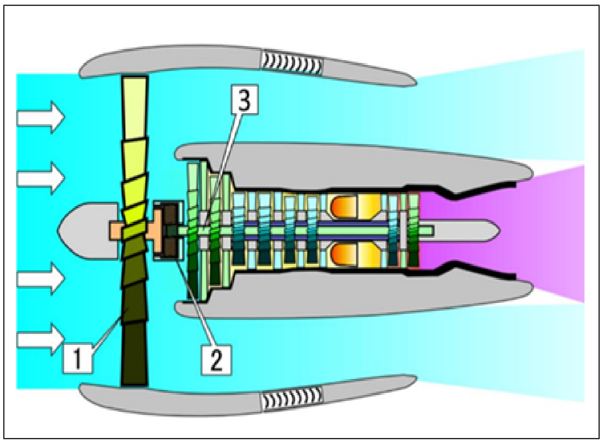

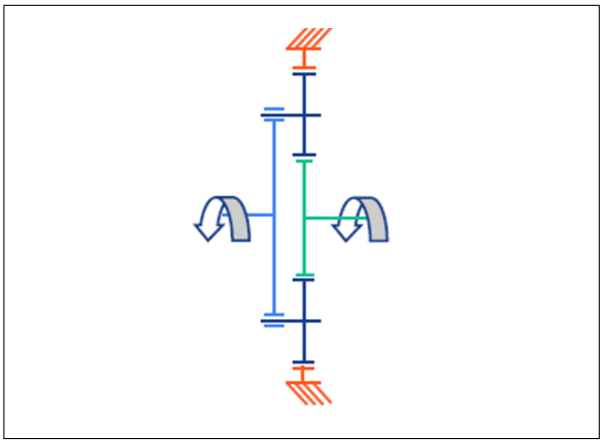

Figure 2: left: the architecture of a next-generation UHBR aircraft engine equipped with an epicyclic gearbox (source: Wikipidia); right : a schematic representation of a planetary gearbox supported hydrodynamic journal bearings.

2.2 Role of the Bearing in Aircraft Engines

To improve the efficiency of next-generation Ultra High Bypass Ratio (UHBR) turbofan engines (Figure 2), it is essential to increase the bypass ratio, which corresponds to the ratio between the cold air that bypasses the engine and the air that flows through the combustion chamber. This ratio mainly depends on the fan diameter: performance improves as the ratio increases. However, an excessive increase in diameter can lead to supersonic blade tip speeds, which may weaken the fan turbine's blades (No.1, Figure2, left).

To overcome this issue, a planetary gearbox is placed between the fan and the low-pressure (LP) shaft (No. 1 and No. 3, Figure 2, left), allowing the fan to operate at a lower speed while maintaining a high rotational speed for the turbine via the LP shaft. In fact, a planetary gearbox (Figure 2, right) is generally selected to optimize the reduction ratio.

The planet gear in planetary gearboxes, subjected to high loads and significant speeds during various flight phases, undergoes deformation due to centrifugal forces and gear meshing. Consequently, rolling-element bearings are unsuitable because of their sensitivity to these stresses and are therefore replaced by hydrodynamic journal bearings with a fixed shaft and rotating bushing (Figure 1), providing effective support through a lubricating oil film.

As part of this work, a computational tool for hydrodynamic journal bearings, incorporating scratches on the surfaces of the shaft (or the bushing), is currently under development. These scratches, caused by abrasive particles originating from manufacturing processes or assembly/disassembly operations, are analyzed based on several parameters: number, orientation, position, depth, and width. The objective is to assess their impact on bearing performance and their role in its degradation. To evaluate the reliability of bearings with respect to this type of defect, a sensitivity analysis is carried out to identify the most influential parameters, by integrating these variables into the dedicated scratched-bearing computational tool [12].

3 SENSITIVITY ANALYSIS OF FAILURE MODES IN HYDRODYNAMIC BEARINGS

3.1 Morris screening Method

The Morris method [7], classified as a screening method, is based on a quasi-random One-At-A-Time (OAT) approach, in which only one input parameter is perturbed at a time by a predefined quantity Δ. Multiple trajectories (r) are generated to efficiently explore the parameter space and assess the influence of each variable on the model response. The principle of the Morris method is relatively simple: each input parameter X_i is defined within an interval $[X_i^{\min}, X_i^{\max}]$, discretized into p levels. A normalized grid is then constructed over the interval $[0, 1]$, and Δ is selected as a multiple of the discretization step $1/(p-1)$. The elementary effect (EE_i) of a parameter—essentially a local gradient—is defined as the change in the model output Y resulting from a perturbation in X_i, as follows:

$$EE_i = \frac{Y(\mathbf{V} + \mathbf{I}_i\Delta) - Y(\mathbf{V})}{\Delta} \tag{3}$$

Where:

- $\mathbf{V} = (X_1, ..., X_{i-1}, X_i, X_{i+1}, ..., X_n)$ is a vector from the matrix of normalized trajectories.
- $\mathbf{V} + \mathbf{I}_i\Delta = (X_1, ..., X_{i-1}, X_i + \varepsilon\Delta, X_{i+1}, ..., X_n)$ is the same vector after perturbation of the i^{th} parameter.
- ε represents the sign of the perturbation, randomly chosen between $+1$ and -1, ensuring that the variation of X_i is either positive or negative.

It is important to note that the value of $\varepsilon\Delta$ is constrained by the condition that the element $X_i + \varepsilon\Delta$ must lie within the interval $[0, 1]$. This constraint justifies the use of the term "quasi-random"; although the sign of the perturbation is initially randomly determined, it can be adjusted to ensure that $X_i + \varepsilon\Delta$ does not exceed the defined bounds. In other words, each parameter is perturbed either upward or downward, but always within the limits of the normalization space.

Campolongo et al. [8] improved the Morris method by introducing an approach based on orientation matrices $\widetilde{\mathcal{O}}^*$, of dimension $(n + 1) \times n$, where n is the number of analyzed parameters. Each column represents a parameter, and each row $\widetilde{\mathbf{V}}_j$ is a trajectory in the normalized space (i.e., one model evaluation). The construction of these matrices follows a sequential process:

- The initial point $\widetilde{\mathbf{V}}_0$ (also called the reference point) is generated by randomly sampling values for each parameter from the discretized grid $\widetilde{\Omega}$ associated with it.
- The first perturbed point $\widetilde{\mathbf{V}}_1$ is obtained by perturbing the first parameter $\widetilde{X}_1$, i.e., $\widetilde{\mathbf{V}}_1 = \widetilde{\mathbf{V}}_0 + \mathbf{I}_1\Delta$.
- The matrix $\widetilde{\mathcal{O}}^*$ is then constructed by successively perturbing only one parameter at a time (hence the OAT principle), following the rule $\widetilde{\mathbf{V}}_{j\neq 0} = \widetilde{\mathbf{V}}_{j-1} + \mathbf{I}_{i=j}\Delta$, thereby ensuring systematic exploration of the parameter space.

To improve the robustness of the analysis, several orientation matrices r are generated. A higher value of r increases the accuracy of the results but also raises the computational cost by increasing the number of model evaluations, defined as $N_c = r \times (n+1)$. In practice, $r = 10$ to 15 is recommended to avoid computational overload of the model.

Each input parameter X_i has a finite distribution $\mathcal{D}_i$ of elementary effects EE_i, composed of r values. Two statistics characterize these effects, Morris [7] proposed computing the mean μ_i and the standard deviation σ_i of $\mathcal{D}_i$ as follows:

$$\mu_i = \frac{1}{r}\sum_{k=1}^{r} EE_i^k \tag{4}$$

$$\sigma_i = \sqrt{\frac{1}{r}\sum_{k=1}^{r}(EE_i^k - \mu_i)^2} \tag{5}$$

In their 2007 study, Campolongo *et al.* [9] analyzed the sensitivity of non-monotonic models, where model outputs may vary between positive and negative values. To better characterize such variations, they introduced the mean of the absolute values of the elementary effects, denoted μ_i^*, defined as:

$$\mu_i^* = \frac{1}{r}\sum_{k=1}^{r} |EE_i^k| \tag{6}$$

The sensitivity analysis derived from Equation (4) allows evaluating the direct impact of an input parameter X_i on the model response Y. Indeed, the higher the mean of the absolute elementary effects μ_i^*, the greater the influence of X_i on the output. Conversely, a low value of μ_i^* indicates a negligible effect. The standard deviation σ_i provides information about the nonlinearity of the relation between X_i and Y, as well as possible interactions between X_i and other parameters $X_{j\neq i}$. A high value of σ_i indicates either a nonlinear relation or a strong interaction with other parameters.

3.2 Variance Decomposition Method

The global sensitivity method is based on the estimation of Sobol indices [10] through the variance decomposition. However, computing these indices requires a large number of samples over the input space and the use of Monte Carlo simulations. Direct use of the numerical model for estimating Sobol indices is impractical due to the significant computational time required. To address this, a surrogate model is built using a Latin Hypercube Sampling (LHS) design of experiments. Sobol indices are then estimated using a Kriging surrogate model [13].

The first-order Sobol index S_i allows the evaluation of the main effect of an input variable X_i on the output Y, excluding interactions with other parameters. It is defined as follows:

$$S_i = \frac{Var(\mathbb{E}(Y|X_i))}{Var(Y)} \tag{7}$$

To evaluate interactions between input parameters, higher-order Sobol indices are introduced. For instance, the second-order index S_{ij} quantifies the effect of the interaction between two input variables X_i and X_j, neglecting their individual effects. It is given by:

$$S_{ij} = \frac{Var(\mathbb{E}(Y|X_i, X_j))}{Var(Y)} - S_i - S_j \tag{8}$$

Thus, S_{ij} measures the combined effect of the two variables X_i and X_j (with $i \neq j$) on the model output, independently of their own main effects.

Finally, the total Sobol index ST_i, which accounts for both the direct effect and all interactions involving X_i, is defined as the sum of the first-order index and all higher-order effects:

$$ST_i = S_i + \sum_{i \neq j} S_{ij} + \dots \tag{9}$$

This total index provides a quantitative measure of the global influence of an input parameter X_i on the output Y, including all interactions with other model inputs.

3.3 Application and Results

We propose in this study to apply the Morris sensitivity analysis method to hydrodynamic journal bearings. The objective is to illustrate the procedure for calculating the elementary effects, as described in the previous section, by applying it to a set of physical parameters influencing the performance of a hydrodynamic journal bearing.

The performance evaluation tool for aeronautical bearings, discussed in the previous section, is used here by neglecting the effects of thermal and elastic deformations. In other words, the developed numerical model only considers a hydrodynamic (HD) modeling framework.

The studied parameters include the geometric dimensions of the bearing and the scratch, as well as the physicochemical, viscous, and thermal properties of the lubricating oil.

We consider a plain hydrodynamic journal bearing with a circumferential scratch on the shaft surface (see Figure 3), defined by its axial position l_s, depth h_s, and width L_s, under the following assumptions:

- The scratch width L_s is assumed to be constant and is considered as a deterministic parameter ($L_s = 0.75\%$ of the bearing length L).
- A single scratch is considered. However, multiple scratches may appear in real conditions.
- The scratch follows a perfectly circumferential path with a uniform depth. However, in real conditions, the scratch depth may vary depending on several factors such as the interaction between the abrasive particle and the moving surfaces, the hardness ratio between the particle and the bearing, *etc.*
- Axial scratches resulting from assembly or manufacturing processes are excluded from this study. Only circumferential scratches with a triangular profile are considered.

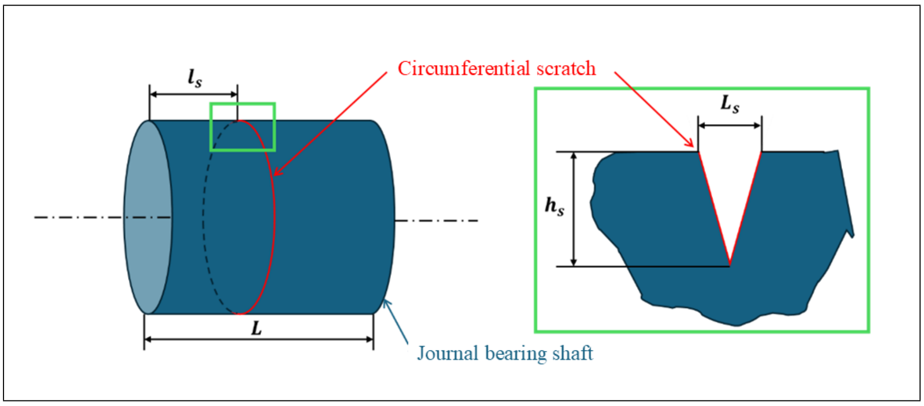

Figure 3: Illustration of the parameters of a circumferential scratch on the surface of a plain hydrodynamic journal bearing shaft.

All studied parameters are listed in Table 1. Specifically, the parameters related to the Morris method are summarized in Table 2. At this stage, it should be noted that the perturbation parameter $\Delta = p/2(p-1)$ follows the expression proposed by Morris [7]. In this study, an additional division by four (i.e., $\Delta = p/8(p-1)$) was introduced to allow a greater number of parameter values within the discretized grid at $p = 16$ levels, evenly distributed between the minimum and maximum values of each parameter. This approach improves the automation process of the Morris method.

In this work, the analysis focuses on the influence of these parameters on the minimum oil film thickness and the maximum pressure, which are considered as performance functions Y_1 and Y_2, respectively. This choice is motivated by the goal of future reliability studies, where these performance functions define the failure criteria of scratched hydrodynamic journal bearings.

Figure 4 shows the ranking of parameters influencing the behavior of a plain journal bearing in an aircraft engine transmission system, in the presence of a circumferential scratch on the shaft surface during the takeoff phase. Two quantities are analyzed: the minimum oil film thickness Y_1 (Figure 4a) and the maximum pressure Y_2 (Figure 4b). Each parameter is represented based on the absolute mean (horizontal axis) and the standard deviation (vertical axis), calculated from Equations (6) and (5), respectively.

Table 1: Input parameters of the aeronautical hydrodynamic journal bearing model

X(N°)	Parameter	Symbol	Unit	Variability
01	Diameter	D	[mm]	Nominal value $\pm$ 1%
02	Length	L	[mm]	Nominal value $\pm$ 1%
03	Radial clearance	C	[μm]	Nominal value $\pm$ 15%
04	Load along x	W_x	[N]	Nominal value $\pm$ 5%
05	Load along y	W_y	[N]	Nominal value $\pm$ 5%
06	Journal rotation speed	V	[rpm]	Nominal value $\pm$ 5%
07	Oil temperature	T	[°C]	Nominal value $\pm$ 35%
08	Oil density	ρ_{oil}	[kg/m^3]	Nominal value $\pm$ 15%
09	Cavitation pressure	p_{cav}	[Pa]	Nominal value $\pm$ 5%
10	Oil heat capacity	C_p	[J/(kg·K)]	Nominal value $\pm$ 15%
11	Carrier radius	R_{PS}	[mm]	Nominal value $\pm$ 1%
12	Carrier rotation speed	V_{PS}	[rpm]	Nominal value $\pm$ 5%
13	Ambient pressure	p_{ambient}	[bar]	Nominal value $\pm$ 10%
14	Supply pressure	p_{supply}	[bar]	Nominal value $\pm$ 15%
15	Axial groove width	L_{groove}	[mm]	Nominal value $\pm$ 1%
16	Groove angle	α	[deg]	Nominal value $\pm$ 1%
17	Groove length	l_{groove}	[mm]	Nominal value $\pm$ 1%
18	Scratch depth	h_s	[μm]	From 0 to 300% of C
19	Axial position of the scratch	l_s	[mm]	From 0 to 50% of L

The analysis highlights three distinct groups of parameters based on their influence on the model response: Group G1 includes parameters exhibiting a nonlinear effect and/or strong interactions with other variables. These parameters have the most significant impact on the model behavior and should be prioritized in uncertainty and reliability analyses. Group G2 consists of parameters with a linear effect and moderate interactions. While their influence is not negligible, it is less dominant than that of G1 parameters, and their contribution is often context-dependent. Group G3 gathers parameters that have a negligible influence on the model response. These can generally be fixed at nominal values without significantly affecting the accuracy of the simulations. Thus, the sensitivity analysis results show that for the minimum oil film thickness (**Figure 4.a**), the oil temperature (X7) is the dominant factor (cf. group G1). A second group of parameters—including the scratch characteristics (depth X18 and position X19), radial clearance (X3), rotation speed (X6), and oil density—exerts an intermediate influence (cf. group G2), while the remaining parameters have a negligible impact (cf. group G3). Regarding the maximum pressure (**Figure 4.b**), the influence hierarchy differs slightly: in addition to oil temperature, the scratch parameters become more influential, showing a marked nonlinear effect. The radial clearance (X3) gains importance, and new parameters enter group G2, notably the applied loads (W_x (X4) and W_y (X5)), the bearing geometry (diameter X1 and length X2), in addition to the rotation speed and oil density. These results help identify the key parameters of the model and distinguish those with negligible effects.

Table 2: Definition of parameters required for the sensitivity analysis using the Morris method

Parameter	Symbol / Expression	Value
Number of input parameters	n	19
Discretization level	p	16
Perturbation	$\Delta = \dfrac{p}{8(p-1)}$	0.13
Number of orientation matrices	r	10
Number of model evaluations	$N_c = r \times (n+1)$	200

To validate the results of the sensitivity analysis obtained using the Morris method, Sobol indices are estimated through a Kriging metamodel built from the 19 input parameters. The design of experiments is generated using a Latin Hypercube Sampling (LHS) technique and is presented in Figure 5. The metamodel is trained and validated using 200 simulations of the numerical bearing model.

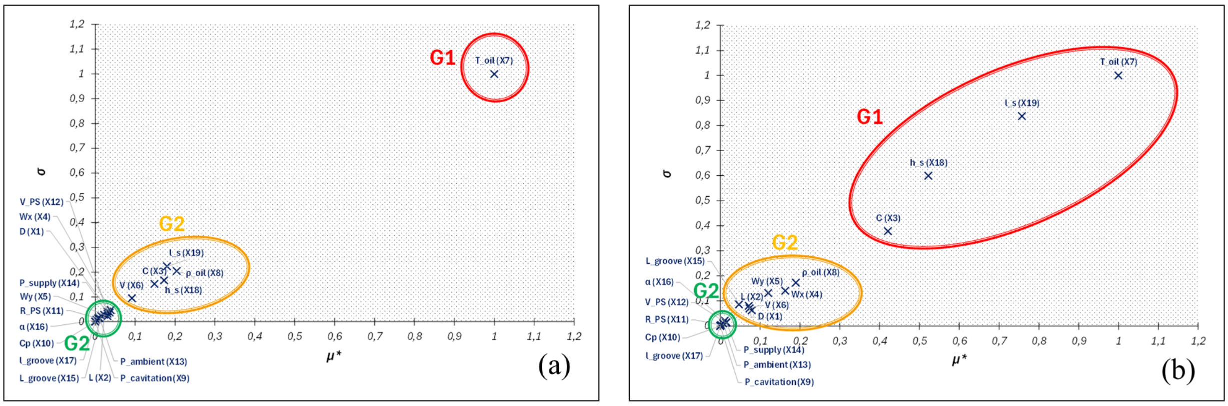

Figure 4: Ranking of the plain bearing model parameters, based on the model response through: (a) minimum oil film thickness – Y_1, (b) maximum pressure – Y_2.

The calculation of first-order Sobol indices (Equation **II.5**) and total-order indices (Equation **II.7**) applied to the metamodel of hydrodynamic journal bearings made it possible to identify, among the 19 studied parameters, those having the greatest impact on both the minimum oil film thickness – Y_1 (Figure 6.a) and the maximum pressure – Y_2 (Figure 6.b). An index close to 1 indicates a significant effect of the parameter on the model output, whereas a low index reflects a negligible impact.

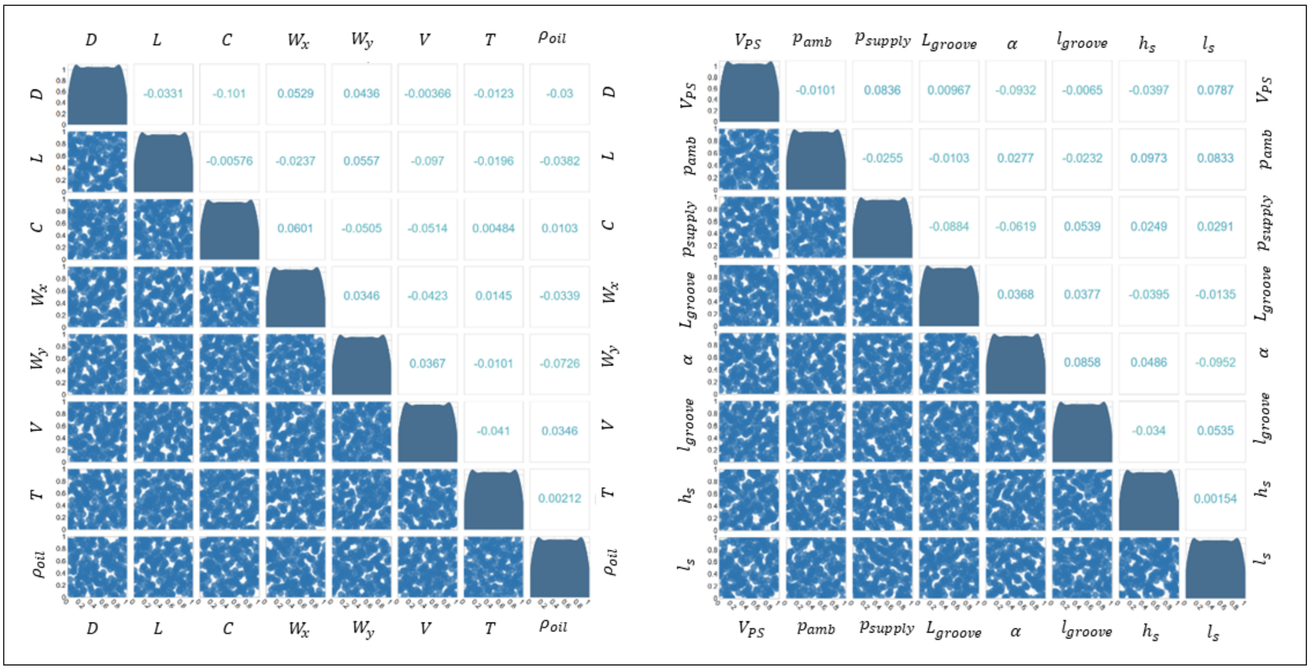

Figure 5: A Latin Hypercube Sampling (LHS) design of experiments generated with 200 sample points in the parameter space of a scratched hydrodynamic bearing.

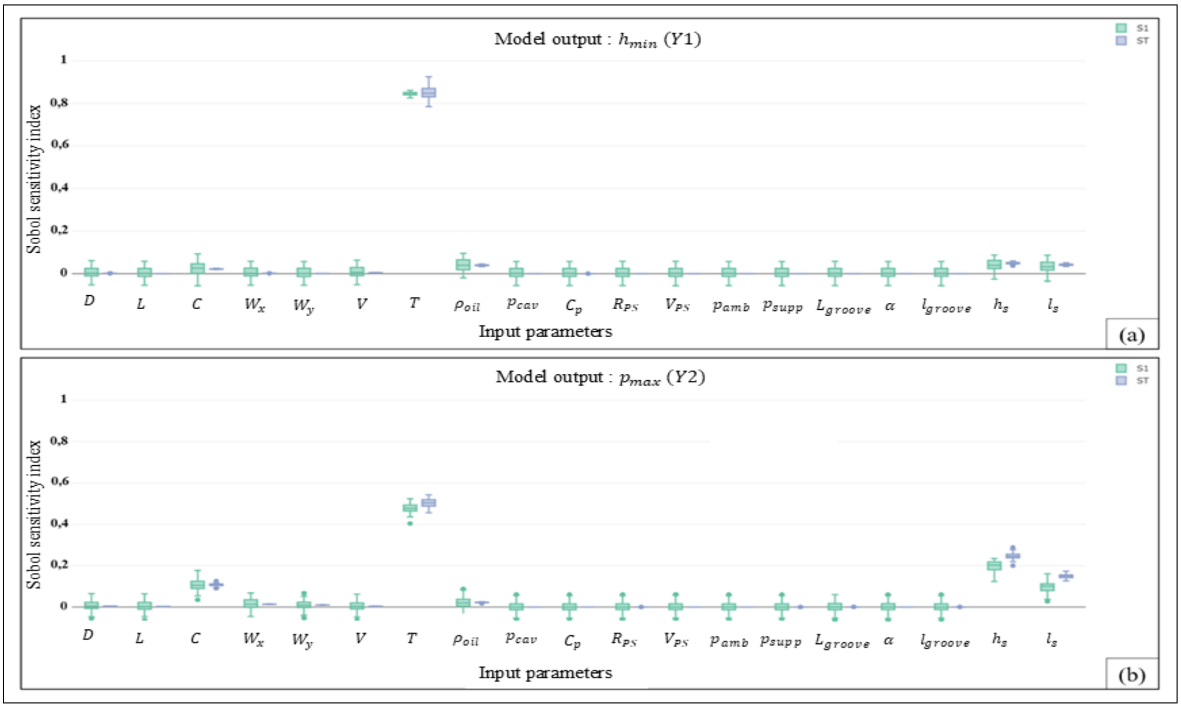

Figure 6: Sensitivity analysis of scratched hydrodynamic bearing parameters using first-order Sobol indices (S1) and total sensitivity indices (ST).

4 CONCLUSIONS AND PERSPECTIVES

The sensitivity analysis of the input parameters of the numerical model for hydrodynamic journal bearings used in aircraft transmission systems has made it possible to identify the main factors likely to influence their reliability. Among them are the oil temperature, the depth and axial position of the circumferential scratch, as well as variations in operating conditions and radial clearance. These parameters significantly affect the minimum fluid film thickness and the maximum hydrodynamic pressure, showing nonlinear effects and/or strong interactions with other model parameters.

Both sensitivity analyses used in this study also revealed parameters that have a negligible influence on bearing performance. This paves the way for reducing the complexity of the reliability problem by limiting the number of random variables to be considered. Such simplification is essential for improving uncertainty propagation studies in the numerical model and conducting more accurate and less computationally expensive reliability analyses.

Finally, several directions for improvement are considered in this study:

- Refining the modeling of scratches by including additional input parameters such as their number, shape, and orientation.
- Investigating the sensitivity analysis of input parameters in the ThermoElastoHydroDynamic (TEHD) model, in order to account for elastic and thermomechanical deformations. This modeling approach requires multiphysical coupling (mechanics, thermal, and hudrodynamics) and is better reflects the real operating conditions of hydrodynamic bearings.
- Performing sensitivity analysis of the TEHD model using variance-based decomposition methods, including the estimation of Sobol indices and/or the FAST method (Fourier Amplitude Sensitivity Test).
- Validating the conclusions through experimental testing.

REFERENCES

[1] M. M. Khonsari and S. H. Wang, “On the role of particulate contamination in scuffing failure,” *Wear*, vol. 137, no. 1, pp. 51–62, Apr. 1990, doi: 10.1016/0043-1648(90)90017-5.

[2] M. B. Dobrica and M. Fillon, “Performance degradation in scratched journal bearings,” *Tribology International*, vol. 51, pp. 1–10, Jul. 2012, doi: 10.1016/j.triboint.2012.02.003.

[3] C. Giraudeau, J. Bouyer, M. Fillon, M. Hélène, and J. Beaurain, “Experimental study of the influence of scratches on the performance of a two-lobe journal bearing,” *Tribology Transactions*, vol. 60, no. 5, pp. 942–955, Sep. 2017, doi: 10.1080/10402004.2016.1238528.

[4] B. Tower, “First Report on Friction Experiments,” *Proceedings of the Institution of Mechanical Engineers*, vol. 35, no. 1, pp. 29–35, Jun. 1884, doi: 10.1243/PIME_PROC_1884_035_013_02.

[5] O. Reynolds, “IV. On the theory of lubrication and its application to Mr. Beauchamp Tower’s experiments, including an experimental determination of the viscosity of olive oil,” *Philosophical Transactions of the Royal Society of London*, vol. 177, pp. 157–234, Jan. 1897, doi: 10.1098/rstl.1886.0005.

[6] O. Reynolds, "IV. On the theory of lubrication and its application to Mr. Beauchamp Tower's experiments, including an experimental determination of the viscosity of olive oil," *Philosophical Transactions of the Royal Society of London*, vol. 177, pp. 157–234, Jan. 1897, doi: 10.1098/rstl.1886.0005.

[7] M. D. Morris, "Factorial sampling plans for preliminary computational experiments," *Technometrics*, vol. 33, pp. 161–174, 1991.

[8] F. Campolongo and R. D. Braddock, "The use of graph theory in the sensitivity analysis of the model output: a second order screening method," *Reliability Engineering & System Safety*, vol. 64, pp. 1–12, 1999.

[9] F. Campolongo, J. Cariboni, and A. Saltelli, "An effective screening design for sensitivity analysis of large models," *Environmental Modelling & Software*, vol. 22, pp. 1509–1518, 2007.

[10] I. Sobol, "Sensitivity estimates for nonlinear mathematical models," *Mathematical Modeling & Computational Experiments*, vol. 1, pp. 407–414, 1993.

[11] H. Riahi, *Analyse de structures à dimension stochastique élevée : application aux toitures bois sous sollicitation sismique*, PhD thesis, 2013.

[12] B. Pap, M. Fillon, M. Guillemont, M., et al. " Experimental and numerical analysis on the seizure of a carbon-filled PTFE central groove journal bearing during start-up period, " *Lubricants*, vol, 6(1), pp 14,2018.

[13] B. Sudret. " Global sensitivity analysis using polynomial chaos expansions," *Reliability engineering & system safety*, vol, 93(7), pp 964–979, 2008.